PHYSICAL REVIEW A VOLUME 25, NUMBER 6 JUNE 1982

Two-photon transitions to excited states in atomic hydrogen

A. Quattropani
Institut de Physique Théorique, Ecole Polytechnique Fédérale de Lausanne, PHB-Ecublens, Confoederatio Helvetica-1015, Lausanne, Switzerland

F. Bassani* and Sandra Carillo
Istituto di Fisica, Università di Roma, I-00185 Roma, Italy
(Received 1 October 1981)

Resonant two-photon transition rates from the ground state of atomic hydrogen to *ns* excited states have been computed as a function of photon frequencies in the length and velocity gauges in order to test the accuracy of the calculation and to discuss the rate of convergence over the intermediate states. The dramatic structure of the transition rates produced by intermediate-state resonances is exhibited. A two-photon transparency is found in correspondence to each resonance.

I. INTRODUCTION

Two-photon spectroscopy has become a very powerful tool for the study of the excitation level of atoms, molecules, and solids.[1] In particular, the great advantage obtained by using counterpropagating beams to eliminate the Doppler broadening has allowed determination of energy levels with much greater precision than in one-photon spectroscopy.[2]

Two-photon transitions have been induced in various types of atoms, particularly Na[3] and Cs,[4] where the optical (*ns*) electron is excited to higher *s* or *d* states or above the ionization threshold. A resonance enhancement of many orders of magnitude has been observed in all alkali atoms when the frequency of one of the photons corresponds to the energy of an intermediate state. The hyperfine splitting has been observed in the initial and final states and also in the intermediate state.[5]

As in all the spectroscopic problems, the case of hydrogen is particularly significant because exact calculations can be carried out and a detailed comparison between theory and experiment can be made on the transition probability as well as on the energies. So far, only the two-photon transition from the ground state to the 2*s* state has been studied both experimentally[6] and theoretically.[7] The Lamb shift of the 1*s* state and the hyperfine splitting have been observed, though a comparison between theoretical and experimental transition rates has not been possible. Two-photon transitions from metastable excited states have also been considered recently.[8]

With the advent of synchroton radiation and the increase in power of the laser beam, it has now become possible, in principle, to measure two-photon absorption coefficients for hydrogen transitions from the ground state to all excited states. For this reason, we think it is of interest to compute the corresponding transition probabilities from the ground state to all excited states. The exact eigenfunctions of the Schrödinger equation are consistently used, while relativistic effects, hyperfine splittings, and the Lamb shift can be taken into account in the energies of the levels. Both the length and velocity gauges are used to check the accuracy of the results by their agreement and to learn the rate of convergence over intermediate states.[7]

We compute the two-photon transition rates to all *ns* excited states as well as to the ionization limit as a function of the photon frequencies. We find a very strong dependence on the frequency of the photons with a resonance enhancement in correspondence to every intermediate state *np* and a transparency frequency before each resonance.

We organize the material as follows: In Sec. II, we describe the general procedure in both length and velocity gauge; in Sec. III, we give the relevant matrix elements in closed form; in Sec. IV, we describe the results for the transition rates to a number of cases of particular interest; in Sec. V, we discuss the phenomena of resonance enhancement and two-photon transparency; in Sec. VI, we discuss the detailed structure of the resonance, including relativistic effects and radiation shifts; in Sec. VII, we obtain and discuss the two-photon ionization limit; and in Sec. VIII, we give conclusions and suggest possible experiments.

II. TWO-PHOTON TRANSITIONS FROM THE GROUND STATE OF HYDROGEN

The two-photon transition rates from the ground state of atomic hydrogen to an excited state ns of the discrete spectrum reads in any gauge j and in the dipole approximation

$$W_1^n=\frac{e^4a_0^4\,|\,E_1^0E_2^0\,|^2}{36(2\pi\hbar^2)^2R^3}\,|\,D_1^n[j]\,|^2\delta(\Delta\nu)\ . \tag{1}$$

The dimensionless transition amplitude $D_1^n[j]$ is separated as

$$D_1^n[j]=D_1^{nd}[j]+D_1^{nc}[j]\ ,$$

where D_1^{nd} and D_1^{nc} are the contributions from the summation on discrete and continuum spectrum, respectively.

The gauge invariance of any physical observable requires that $D_1^n[j]$ be independent of the particular gauge.[9] In an explicit calculation, care must be taken to preserve gauge invariance, in particular, when approximations are adopted.[10] In the particular case of atomic hydrogen, the complete set of exact eigenstates can be used in order to evaluate $D_1^n[j]$. Furthermore, we adopt the dipole approximation in describing the electromagnetic field and we make explicit calculations in two different gauges, the length gauge J_0 and the velocity gauge J. The electron-photon interaction is given in the gauges J_0 and J by

$$h_{J_0}^{\rm int}=e\Phi(\vec{x},t)=-eE_0^{(1)}\hat{e}_1\cdot\vec{x}(e^{i\omega_1t}+\text{c.c.})-eE_0^{(2)}\hat{e}_2\cdot\vec{x}(e^{i\omega_2t}+\text{c.c.}) \tag{2a}$$

and

$$h_J^{\rm int}=-\frac{e}{mc}\vec{A}(t)\cdot\vec{p}=\frac{ie}{m}\left[\frac{E_0^{(1)}}{\omega_1}(e^{i\omega_1t}-\text{c.c.})\hat{e}_1\cdot\vec{p}+\frac{E_0^{(2)}}{\omega_2}(e^{i\omega_1t}-\text{c.c.})\hat{e}_2\cdot\vec{p}\right]\ . \tag{2b}$$

In the gauges J_0 and J the transition amplitudes D_1^{nd} and D_1^{nc} read

$$D_1^{d,n}[J_0]=\tfrac{1}{2}\sum_{\mu=2}^{\infty}[(1-1/\mu^2-\nu_1)^{-1}+(1/n^2-1/\mu^2+\nu_1)^{-1}]R_{10}^{\mu1}R_{n0}^{\mu1}\ , \tag{3a}$$

$$D_1^{c,n}[J_0]=\tfrac{3}{2}\int_0^{\infty}dw[(2w+1-\nu_1)^{-1}+(2w+1/n^2+\nu_1)^{-1}]R_{10}^{w1}R_{n0}^{w1}\ , \tag{3b}$$

$$D_1^{d,n}[J]=-\tfrac{1}{2}\sum_{\mu=2}^{\infty}[(1-1/\mu^2-\nu_1)^{-1}+(1/n^2-1/\mu^2+\nu_1)^{-1}]R_{10}^{\mu1}R_{n0}^{\mu1}$$
$$\times(1-1/n^2)(1/n^2-1/\mu^2)[\nu_1(1-1/n^2-\nu_1)]^{-1}\ , \tag{3c}$$

$$D_1^{c,n}[J]=-\tfrac{3}{2}\int_0^{\infty}dw[(2w+1-\nu_1)^{-1}+(2w+1/n^2+\nu_1)^{-1}]R_{10}^{w1}R_{n0}^{w1}$$
$$\times(1+2w)(1/n^2+2w)[\nu_1(1-1/n^2-\nu_1)]^{-1}\ , \tag{3d}$$

where R_{n0}^{w1} and $R_{n0}^{\mu1}$ are the matrix elements of r/a_0, appropriate to intermediate states belonging to continuous and discrete spectrum, respectively. In (1) and (2), a_0 denotes the Bohr radius, $\hat{e}_1,\hat{e}_2$ the polarization unit vectors of the incident beams of amplitudes $E_0^{(1)},E_0^{(2)}$, and frequencies $\omega_1=R\nu_1,\omega_2=R\nu_2$, R being the Rydberg frequency. The energies of the discrete and continuum spectrum are $\hbar R\nu(\mu)=-\hbar R/\mu^2$ and $2w\hbar R>0$, respectively.

From now on, we take both beams to be polarized in the z direction, so that only the states with angular momentum $l=1$ and $m=0$ have to be considered in the summation over the intermediate states. Because of the spherical symmetry of s states, this transition probability has to be multiplied by a factor $\cos^2(\Theta)$, when the two beams are polarized with a relatvie angle Θ. This gives a factor of $\frac{1}{2}$ for unpolarized light, the direction of propagation being generally fixed in an absorption experiment.

In order to verify the accuracy of the calculation and to assess the relative importance of different energy ranges in the summation over intermediate states, we compute separately $D_1^n[J]$ and $D_1^n[J_0]$ for all $|n00\rangle$ final states of the discrete spectrum.

III. COMPUTATION OF THE DIPOLE MATRIX ELEMENTS

The matrix elements $R_{n0}^{\mu 1}$ for $n \neq \mu$, have been computed from the following expression obtained by Gordon[11] and reported by Bethe and Salpeter[12]:

$$R_{n0}^{\mu 1} = \frac{(-1)^{\mu-1}}{4} \left[\frac{(n+1)!\mu!}{(n-2)!(\mu-1)!} \right]^{1/2} \frac{(4n\mu)^2 (n-\mu)^{\mu+n-2}}{(n+\mu)^{n+\mu}}$$
$$\times \left[F\left[-n+2; -\mu+1; 2; -\frac{4n\mu}{(n-\mu)^2} \right] - \left[\frac{n-\mu}{n+\mu} \right]^2 F\left[-n; -\mu-1; 2; \frac{-4n\mu}{(n-\mu)^2} \right] \right], \tag{4a}$$

where $F(\alpha;\beta;\gamma;x)$ is the hypergeometric function defined, e.g., in Bethe and Salpeter,[12] Eq. (63.3).

For $n = \mu$ the simple expression

$$R_{n0}^{n1} = -\tfrac{3}{2} n (n^2-1)^{1/2} \tag{4b}$$

holds. We notice that the negative sign is missing in expression (63.5) given in Bethe and Salpeter.[12] For large values of the principal quantum number μ and for all n, the following asymptotic expression holds:

$$R_{n0}^{\mu 1} \simeq \mu^{-3/2} \tfrac{4}{3} n^{7/2} e^{-2n} \sum_{k=0}^{n-1} \frac{(1-n)_k}{(2)_k} 2^k (k+1)_4 F(-k-1;4;2n)$$
$$\simeq c(n) \mu^{-3/2} , \tag{4c}$$

with

$$(n)_k \equiv n(n+1)(n+2)\cdots(n+k-1) ,$$

and where $F(\alpha;\beta;x)$ is the usual confluent hypergeometric function [see, e.g., Bethe and Salpeter,[12] Eq. (3.4)]. We observe that care must be taken in using expression (4c) for large n. For large values of n, expression (4c) becomes

$$c(n) \sim \frac{1}{128 n^{3/2}} \int_0^\infty J_1(r) r^5 dr . \tag{4d}$$

The dipole matrix element R_{n0}^{w1} between a discrete state $|n00\rangle$ and a state of the continuum $|w10\rangle$ is computed analytically using the procedure of Sommerfeld and Schur.[13] We obtain

$$R_{n0}^{w1} = \frac{\exp[-(2/\sqrt{2w})\arctan(n\sqrt{2w})]}{16w[1-\exp(-2\pi/\sqrt{2w})]^{1/2}} \left[\frac{n(2w+1)}{w} \right]^{1/2} \left[\frac{4n\sqrt{2w}}{1+n^2 2w} \right]^2$$
$$\times \left| \left[\frac{1+in\sqrt{2w}}{1-in\sqrt{2w}} \right]^{n-2} F\left[2-\frac{i}{2w}; 1-n; 2; \frac{4in\sqrt{2w}}{(1+in\sqrt{2w})^2} \right] \right.$$
$$\left. - \left[\frac{1+in\sqrt{2w}}{1-in\sqrt{2w}} \right]^{n} F\left[-\frac{i}{\sqrt{2w}}; 1-n; 2; \frac{4in\sqrt{2w}}{(1+in\sqrt{2w})^2} \right] \right| . \tag{5}$$

IV. TRANSITION RATES

Using the computed dipole matrix elements, we calculate the dimensionless transition amplitudes[3] for $1s$-ns two-photon transitions. The sum over the discrete states $|\mu 10\rangle$ is carried out term by term up to an appropriate value N, which depends on the final state $|n00\rangle$ and by integration for $\mu > N$. The substitution of the discrete sum by an integral gives results as accurate as 0.1%. The contribution of the intermediate states belonging to the continuum is evaluated by numerical integration.

In Table I, we report the values of the transition amplitudes $D_1^n[J_0]$ and $D_1^n[J]$ for transitions to final states $|n00\rangle$, with $n=3,6,20$ as a function of the frequency ω_1 of one of the incoming beams. The frequency ω_2 is given by energy conservation as

$$\hbar\omega_2 = E_{n0} - E_{10} - \hbar\omega_1 \ . \tag{6}$$

It can be observed that the computations performed in the length and velocity gauge give results in total agreement. However, the role of the discrete and continuum spectrum is dramatically different in the two gauges. In particular, in the gauge J_0 the largest contribution in the summation arises from the intermediate state with $\mu=n$, because of the large value of the dipole matrix ele-

TABLE I. (a) Dimensionless two-photon transition rate amplitudes $D_1^3[J_0]$ and $D_1^3[J]$ for $1s$-$3s$ transition in hydrogen for a number of values of ν_1 in the length and velocity gauge, respectively. D_1^{3d} and D_1^{3c} denote the contributions from the discrete and continuum spectrum, respectively. (b) Same as (a) for the $1s$-$6s$ transition. (c) Same as (a) for the $1s$-$20s$ transition.

ν_1	$D_1^3[J_0]^d$	$D_1^3[J_0]^c$	$D_1^3[J_0]$	$D_1^3[J]^d$	$D_1^3[J]^c$	$D_1^3[J]$
			(a)			
0.3750	−5.4479	2.2125	−3.2354	0.5605	−3.7960	−3.2354
0.6750	−4.1756	2.5063	−1.6693	3.8444	−5.5137	−1.6693
0.6875	−3.2446	2.5483	0.6963	5.1183	−5.8146	0.6963
0.7000	−1.6096	2.5943	0.9847	7.1475	−6.1628	0.9847
0.7125	1.5137	2.6446	4.1583	10.7269	−6.5686	4.1583
0.7250	8.5166	2.6996	11.2162	18.2615	−7.0453	11.2162
0.7375	31.4663	2.7600	34.2263	41.8371	−7.6107	34.2263
0.7475	224.0014	2.8125	226.8139	234.9570	−8.1431	226.8139
0.7650	−61.1148	2.9147	−58.2000	−48.8976	−9.3024	−58.2000
0.8000	−41.4777	3.1678	−38.3099	−25.1949	−13.1150	−38.3099
0.8250	−49.9815	3.4019	−46.5797	−28.0138	−18.5659	−46.5797
0.8500	−78.1203	3.6999	−74.4204	−43.0919	−31.3285	−74.4204
0.8750	−224.0759	4.0912	−219.9846	−128.7985	−91.1861	−219.9846
0.8860	−1121.5411	4.3051	−1117.2360	−669.9164	−448.0724	−1117.2361
ν_1	$D_1^6[J_0]^d$	$D_1^6[J_0]^c$	$D_1^6[J_0]$	$D_1^6[J]^d$	$D_1^6[J]^c$	$D_1^6[J]$
			(b)			
0.4860	−3.5678	2.8154	−0.7524	0.7415	−1.4938	−0.7523
0.6750	−3.4440	3.1723	−0.2717	1.6316	−1.9032	−0.2716
0.7000	−3.0060	3.2911	0.2851	2.3378	−2.0526	0.2852
0.7250	−1.2564	3.4363	2.1799	4.4249	−2.2449	2.1799
0.7475	35.1736	3.5948	38.7684	41.2361	−2.4671	38.7690
0.7525	−46.5525	3.6342	−42.9183	−40.3933	−2.5244	−42.9177
0.7800	−9.5969	3.8841	−5.7128	−2.8052	−2.9074	−5.7126
0.8000	−8.6193	4.1087	−4.5107	−1.2284	−3.2820	−4.5105
0.8500	−8.1031	4.9127	−3.1903	1.6987	−4.8889	−3.1901
0.8750	−3.2078	5.5265	2.3187	8.7623	−6.4434	2.3189
0.8860	36.1922	5.8695	42.0617	49.5225	−7.4600	42.0624
0.8900	−148.4926	6.0086	−142.4840	−134.5755	−7.9065	−142.4820
0.9000	−29.8864	6.3972	−23.4893	−14.2202	−9.6863	−23.4888
0.9200	−21.3657	7.4097	−13.9560	−0.1709	−13.7848	−13.9557
0.9350	62.4806	8.4894	70.9700	91.7405	−20.7691	70.9714
0.9400	−160.0602	8.9430	−151.1172	−126.4391	−24.6759	−115.1149
0.9500	−78.2764	10.0575	−68.2189	−30.0409	−38.1767	−68.2175
0.9575	84.3860	11.1499	95.5359	156.6250	−61.0861	95.5389
0.9625	−656.7408	12.0573	−644.6836	−574.9131	−96.7605	−644.6736
0.9650	−634.3876	12.5826	−621.8050	−488.2735	−133.5234	−621.7969

TABLE I. (*Continued.*)

ν_1	$D_1^{20}[J_0]^d$	$D_1^{20}[J_0]^c$	$D_1^{20}[J_0]$	$D_1^{20}[J]^d$	$D_1^{20}[J]^c$	$D_1^{20}[J]$
			(c)			
0.4950	−2.8912	2.7824	−0.1088	0.1936	−0.3023	−0.1087
0.7250	−3.1394	3.4466	0.3071	0.7445	−0.4372	0.3072
0.7475	1.7171	3.6281	5.3452	5.8231	−0.4778	5.3453
0.7525	−9.5643	3.6737	−5.8906	−5.4021	−0.4882	−5.8902
0.7800	−4.7289	3.9656	−0.7634	−0.2060	−0.5572	−0.7632
0.8000	−4.8213	4.2325	−0.5888	0.0352	−0.6238	−0.5886
0.8500	−5.6016	5.2213	−0.3803	0.5185	−0.8986	−0.3801
0.8860	−1.9177	6.4619	4.5441	5.8494	−1.3051	4.5443
0.9000	−9.5226	7.1748	−2.3478	−0.7781	−1.5693	−2.3474
0.9200	−9.7726	8.5983	−1.1743	0.9892	−2.1632	−1.1739
0.9400	−20.5128	10.8900	−9.6228	−6.3161	−3.3059	−9.6219
0.9485	−15.8589	12.3523	−3.5065	0.6508	−4.1568	−3.5060
0.9660	−24.3015	17.3789	−6.9226	0.9151	−7.8368	−6.9217
0.9700	−17.7632	19.2463	1.4832	11.0023	−9.5180	1.4843
0.9720	81.4443	20.3551	101.7994	112.4041	−10.6014	101.8027
0.9740	−43.4070	21.6126	−21.7944	−9.8831	−11.9096	−21.7927
0.9760	−34.8986	23.0516	−11.8470	1.6684	−13.5138	−11.8454
0.9780	−24.2734	24.7160	0.4426	15.9613	−15.5173	0.4439
0.9800	−110.8083	26.6649	−84.1434	−66.0645	−18.0750	−84.1395

ment,[4] which has a sign opposite to all other contributions. In the gauge J the intermediate state $\mu=n$ gives zero contribution because of the degeneracy in the energy. It can be observed from the agreement between the two gauges that the accuracy of the computation decreases with increasing value of the principal quantum number of the final state.

A problem that one has to consider in an approximate calculation is the rate of convergence of the sum over the discrete intermediate states and the relative contribution of the continuum. For frequencies out of the condition of resonance enhancement, a heuristic approximation generally adopted is to consider only a limited number of intermediate states, choosing those close to initial and final states because of their smaller energy denominators. For the case of 1*s*-2*s* transition in hydrogen,[7] we have shown that this is well justified in the length gauge J_0. This conclusion cannot be generalized to higher excited states because the contribution of all states from the discrete and continuum spectrum are comparable. Therefore, gauge invariance has to be consistently used as a test of the accuracy of the calculation. Indeed such a test has led to display nonlocal effects in two-photon transitions to exciton states in solids.[10]

V. RESONANCE ENHANCEMENT AND TWO-PHOTON TRANSPARENCY

In order to illustrate the physical significance of the results, we discuss the amplitude of the 1*s*-*ns* transition as a function of ω_1. For

$$\omega_1=R\left[1-\frac{1}{\mu^2}\right]\equiv R\nu^{\mu}(\text{res})\ , \tag{7}$$

with $\mu=2,3,\ldots,n$, the amplitude has a first-order pole, and thus near resonance the amplitude is dominated by the term

$$D_1^n[J_0]\approx\frac{\left\langle n00\left|\frac{z}{a_0}\right|\mu10\right\rangle\left\langle\mu10\left|\frac{z}{a_0}\right|100\right\rangle}{1-\nu_1-\frac{1}{\mu^2}}\ . \tag{8}$$

Since all matrix elements are positive except those with $\mu=n$ all resonances have positive amplitude for $\nu_1\lesssim\nu^{\mu}(\text{res})$ except the last one for which $\mu=n$; futhermore for $\nu_1=\nu_2$ the amplitude D_1^n is negative. Therefore, there exists in correspondence to every resonance with $\mu\leq n-1$ a frequency $\nu_0^{\mu}(2\leq\mu\leq n-1)$, for which the amplitude vanishes; we expect a two-photon transparency to be

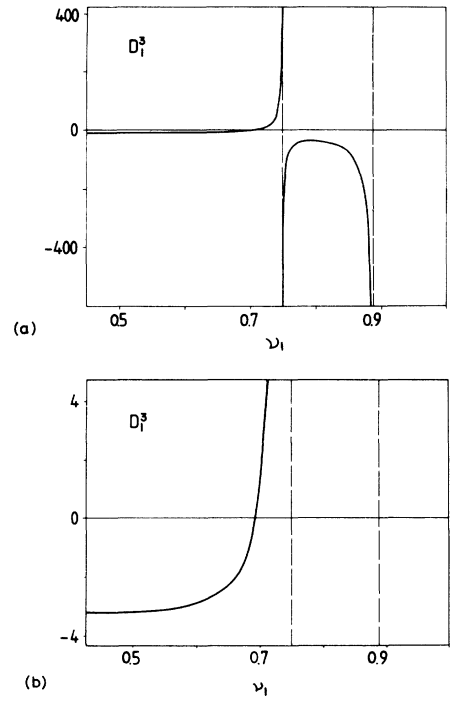

FIG. 1. (a) Two-photon transition amplitude D_1^3 for $1s$-$3s$ transitions as a function of $\omega_1 = R\nu_1$ for $\frac{4}{9} \leq \nu_1 \leq \frac{8}{9}$. (b) Same as (a), but with a magnified vertical scale in order to display the two-photon transparency frequency $\nu_0^{\mu=2}$.

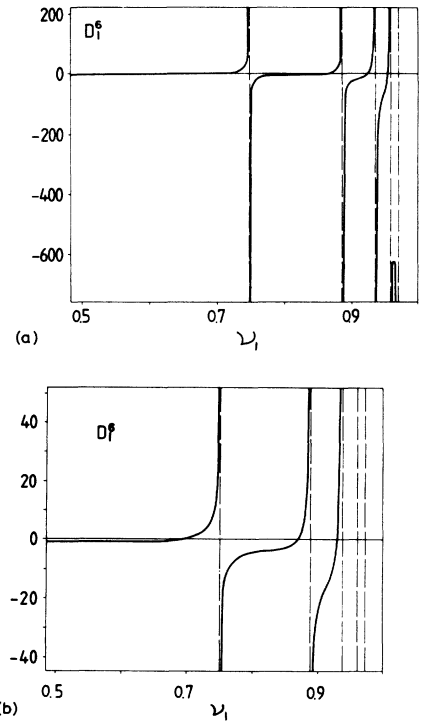

FIG. 2. (a) Two-photon transition amplitude D_1^6 for $1s$-$6s$ transitions as a function of $\omega_1 = R\nu_1$ for $\frac{35}{72} \leq \nu_1 \leq \frac{35}{36}$. (b) Same as (a), but with a magnified vertical scale in order to display the two-photon transparency frequencies ν_0^μ, $\mu = 2,3,4$.

observed at such frequencies. The values of ν_0^μ for the $1s$-$3s$, $1s$-$6s$, and $1s$-$20s$ transitions are given in Table II. For the last case, only the first five transparency frequencies have been calculated.

The above results are clearly displayed in Figs. 1 and 2, where we plot the two-photon transition amplitudes for the $1s$-$3s$ and $1s$-$6s$ transition amplitudes, respectively, as function of ν_1. The dimensionless two-photon absorption coefficient $|D_1^n|^2$ is plotted in Figs. 3 and 4 for the $1s$-$3s$ and $1s$-$6s$ transitions, respectively. Over the entire frequency range the absorption displays a dramatic structure. Besides the resonance enhancement at $\nu_1 = \nu^\mu(\text{res})$, the plots clearly show the two-photon transparency.

The above results and, in particular, the detailed line shape as displayed in Figs. 3 and 4 suggest that two-photon spectroscopy can give new precise information on the excited states of atomic hydrogen. Not only the final state can be determined with great accuracy, but highly precise spectroscopy of intermediate states can be performed. In fact, resonance enhancement is an extremely precise tool since more than a seven order of magnitude variation can be reached.[2]

VI. DETAILED STRUCTURE OF THE RESONANCES

The line shapes described in Sec. V, with sharp resonances at all allowed intermediate states and well-defined photon energies to eliminate Doppler broadening between initial and final states, clearly indicate that the experimental accuracy is suffi-

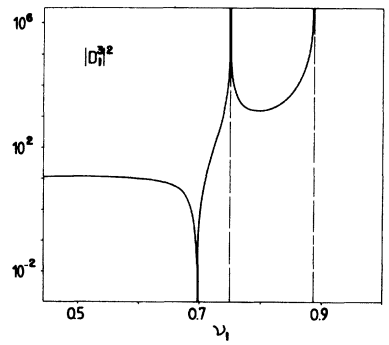

FIG. 3. Dimensionless two-photon absorption coefficient $|D_1^3|^2$ for $1s$-$3s$ transition plotted for $\frac{4}{9} \leq \nu_1 \leq \frac{8}{9}$.

TABLE II. Two-photon transparency frequencies ν_0^{μ} for the 1s-3s, 1s-6s, and 1s-20s two-photon transitions in atomic hydrogen. The ν_0^{μ}, $2 \le \mu \le n-1$ are the solutions of $D_1^n(\nu_1)=0$. For the 1s-20s transitions only the first five values of ν_0^{μ} are reported. Units are in Rydberg frequency.

μ	2	3	4	5	6
$\nu_0^{(\mu)}$(1s-3s)	0.6935				
$\nu_0^{(\mu)}$(1s-6s)	0.6882	0.8675	0.9292	0.9556	
$\nu_0^{(\mu)}$(1s-20s)	0.6895	0.8703	0.9293	0.9551	0.9697

cient to display the internal structure of the resonant intermediate states. This will appear as a multiple resonance of the kind observed by Björkholm[2,5] for the case of sodium.

As an illustrative example we present in Fig. 5 an energy-level scheme relevant to the two-photon transition 1s-3s in hydrogen. Though the transition probabilities can be computed with the states obtained from the Schrödinger equation as we have done, the energies appearing in the initial, final, and in the resonant state at resonance are chosen to include fine-structure Lamb shifts and hyperfine structures. We report in this figure the values of the energies as originating from the Dirac relativistic equation, then we add the Lamb shifts of the s states and the hyperfine splittings due to the nuclear magnetic moment.[14] For a detailed discussion of recent experiments, sufficiently accurate to give the values reported in Fig. 5, we refer to the review articles by Hänsch *et al.*[15] and by Ferguson *et al.*[16] For comparison, we show in Fig. 5 also the 2s level, though it is not relevant to the 1s-3s transition.

The two-photon transition 1s-3s proceeds via the intermediate states

$$nP_{1/2}(F=0,F=1)$$

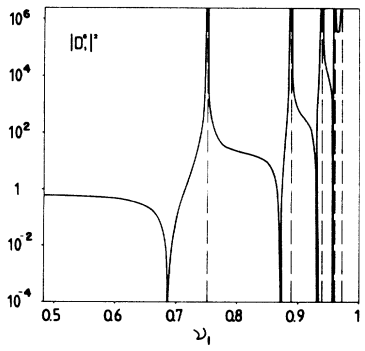

FIG. 4. Dimensionless two-photon absorption coefficient $|D_1^6|^2$ for 1s-6s transition plotted for $\frac{35}{72} \le \nu_1 \le \frac{35}{36}$.

and

$$nP_{3/2}(F=1,F=2)\ ,$$

where resonances can occur. We must take into account the selection rules on the individual matrix elements $\Delta F = \pm 1,0$ with exclusion of $F=0 \rightarrow$

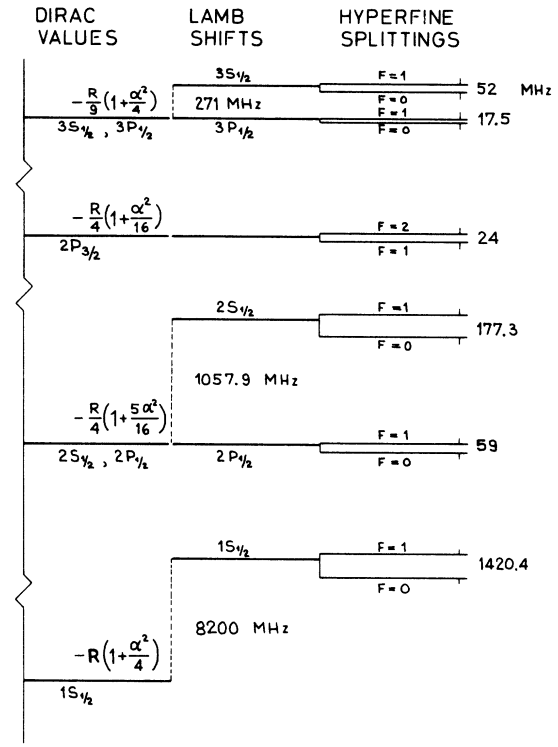

FIG. 5. Schematic energy-level diagram for the lowest states of atomic hydrogen relevant to the 1s-2s and to the 1s-3s two-photon transitions. The relativistic eigenvalues are given on the left side in terms of the fine-structure constant α, the Lamb-shift corrections are reported at the center, and the hyperfine splittings are given on the right side. Numerical values for the hyperfine splittings of p states have been roughly estimated from existing experimental data along lines developed for alkali atoms (Ref. 14).

$F=0$, and the two-photon selection rule for transitions between states $\Delta F^{(2)}=0$ due to the fact that the electron-photon interaction does not operate on electron- and nuclear-spin coordinates.[17] The two allowed two-photon transitions $1S_{1/2}(F=0) \rightarrow 3S_{1/2}(F=0)$ and $1S_{1/2}(F=1) \rightarrow 3S_{1/2}(F=1)$ will be separated by the ground-state hyperfine splitting (1420 MHz), decreased by the hyperfine splitting of the state $3s$ (of the order of 10 MHz). The first transition $F=0 \rightarrow F=0$ will have two allowed resonances in correspondence to the two allowed intermediate states $2P_{1/2}(F=1)$ and $2P_{3/2}(F=1)$, separated by the fine-structure splitting $\alpha^2/16$ in Rydberg units, decreased by about $(\frac{1}{4}59+\frac{5}{8}24)$ MHz. The second transition $F=1 \rightarrow F=1$, will have four allowed resonances, a doublet corresponding to the intermediate states $2P_{1/2}(F=1,F=0)$, and another doublet corresponding to the states $2P_{3/2}(F=2, F=1)$. It is quite conceivable that experimental resolution will be sufficient to detect this structure. Another intermediate state resonance will occur in correspondence to the $3P_{1/2}(F)$ state separated from the final state by the Lamb shift.

In high-resolution two-photon spectroscopy with an intense light beam it is important to account for the shifts of atomic energy levels due to the dynamical Stark effect.[18] These shifts are particularly large in a resonantly enhanced two-photon process, as it was shown by Liao and Björkholm[19] in the case of sodium. The shift ΔE_n of an atomic state $|n\rangle$ induced by the radiation field $\vec{E}=\hat{e}E_0e^{-i\omega t}+\text{c.c.}$ is given by perturbation theory as

$$\Delta E_n=\sum_m \left[\frac{|eE_0|^2|\langle n|\hat{e}\cdot\vec{x}|m\rangle|^2}{E_n-E_m-\hbar\omega}+\frac{|eE_0|^2|\langle n|\hat{e}\cdot\vec{x}|m\rangle|^2}{E_n-E_m+\hbar\omega} \right] . \tag{9}$$

The summation is taken over all unperturbed atomic states $|m\rangle$, but near resonance we may consider in the sum only the term with the smallest energy denominator.

We consider first the $1S_{1/2}(F=0) \rightarrow 3S_{1/2}(F=0)$ transition with ω_1 close to the resonance frequency corresponding to the $2P_{1/2}(F=1)$ intermediate states. For light beams polarized in the z direction the frequency shift of the $1S_{1/2}(F=0)$ level reads

$$\delta\nu[1S_{1/2}(0)|2P_{1/2}(1)](\text{Hz})=1.03\times10^{14}\frac{I(\text{W cm}^{-2})}{\Delta\nu(\text{Hz})}|\langle 1s||x||2p\rangle|^2(\text{a.u.}) , \tag{10}$$

where

$$\Delta\nu=\frac{1}{h}\{E[1S_{1/2}(0)]-E[2P_{1/2}(1)]+\hbar\omega_1\}$$

is the frequency detuning and I the intensity of the beam of frequency ω_1. A similar expression holds for the $3S_{1/2}(0)$ level, but now the radiation to be considered is that of the second laser beam, in this case

$$\Delta\nu=\frac{1}{h}\{E[3S_{1/2}(0)]-E[2P_{1/2}(1)]-\hbar\omega_2\} .$$

We recall that Eq. (10) is valid provided that $\delta\nu \ll \Delta\nu$ and $\Delta\nu$ many times larger than the natural linewidth. As an example for an intensity of 2 kW cm^{-2} and a detuning of 10 GHz the shift of the $1S_{1/2}(0)$ level is of the order of 35 MHz. It is important to notice that this frequency shift is comparable with the hyperfine splitting of the $3S_{1/2}$ state, and therefore can not be neglected in comparing it with the experiment near intermediate-state resonance.

In Table III, we give the relevant matrix elements for the evaluation of the frequency shifts of the $1S_{1/2}(F)$ and $3S_{1/2}(F)$ levels for the resonant enhanced $1S_{1/2}(F) \rightarrow 3S_{1/2}(F)$ two-photon transi-

TABLE III. Relevant matrix elements for the evaluation of the frequency shifts of the $1S_{1/2}(F)$ and $3S_{1/2}(F)$ levels for the resonant enhanced $1S_{1/2}(F) \rightarrow 3S_{1/2}(F)$ two-photon transitions.

Transition	Resonant intermediate states	$\lvert\langle vp \lvert x \rvert 1s\rangle\rvert^2$ (a.u.)	$\lvert\langle vp \lvert x \rvert 3s\rangle\rvert^2$ (a.u.)
$1S_{1/2}(0) \rightarrow 3S_{1/2}(0)$	$2P_{1/2}(1), 2P_{3/2}(1)$	1.665	0.881
$1S_{1/2}(1) \rightarrow 3S_{1/2}(1)$	$2P_{1/2}(0), 2P_{1/2}(1), 2P_{3/2}(1), 2P_{3/2}(2)$	1.665	0.881
	$3P_{1/2}(0), 3P_{1/2}(1)$	0.267	162.0

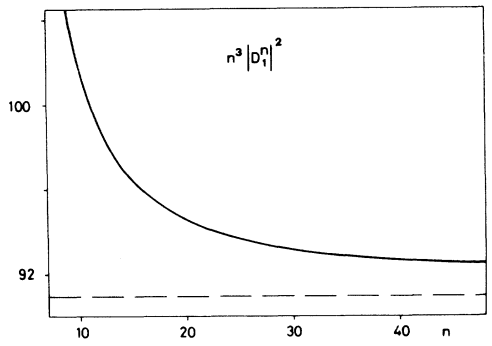

FIG. 6. Rate of convergence of $n^3 | D_1^n |^2$ towards the threshold probability, evaluated in the gauge J for $\nu_1=0.5$.

tions. Similar considerations can be made for deuterium, where the smaller hyperfine splittings can be also detected as they have been in the two-photon transitions $1S_{1/2} \rightarrow 2S_{1/2}$.[16]

VII. IONIZATION LIMIT

In order to evaluate the two-photon threshold probability for ionization one has to consider D_1^n in the limit $n \rightarrow \infty$. The density of final states being $n^3/2R$, the threshold probability is given by

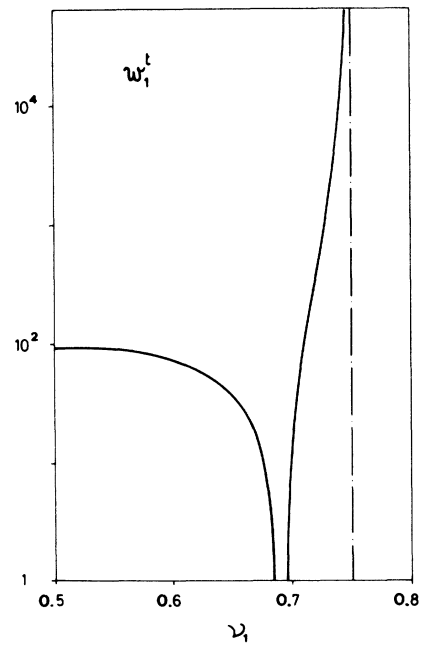

FIG. 7. Dimensionless two-photon threshold probability $w_1^t = \lim_{n\rightarrow\infty} | D_1^n |^2 n^3$ as a function of ν_1.

TABLE IV. Dimensionless two-photon threshold probability $w_1^t = \lim_{n\rightarrow\infty} | D_1^n |^2 n^3$ for a number of frequencies $\nu_1 < 0.75$.

ν_1	$\lvert D_1^n \rvert^2 n^3$ $n=45$	w_1^t
0.7475	2.2259×10^5	2.1755×10^5
0.7425	2.0080×10^4	1.9989×10^4
0.7350	3.5499×10^3	
0.7275	1.0568×10^3	1.0528×10^3
0.7100	8.8970×10	8.8893×10
0.7000	1.4286×10	1.4188×10
0.6900	2.6907×10^{-2}	
0.6800	5.1047	
0.6700	1.6415×10	1.6150×10
0.6600	2.8493×10	2.7881×10
0.6000	7.5727×10	7.4503×10
0.5800	8.2919×10	8.1583×10
0.5000	9.2581×10	9.0964×10

$$W_1^t = \lim_{n\rightarrow\infty} \frac{e^4 a_0 \, | E_1^0 E_0^2 |^2}{36(2\pi\hbar^2)^2 R^2} \, | D_1^n |^2 \frac{n^3}{2R} \, . \qquad (11)$$

For $\omega_1=\omega_2=R/2$ we obtain

$$w_1^t(\nu_1=0.5) = \lim_{n\rightarrow\infty} | D_1^n |^2 n^3 \approx 90.9 \, .$$

The threshold probability can also be obtained as the limit of the two-photon ionization for zero-electron momentum using the procedure described by Rahman.[20]

In Fig. 6, we display $| D_1^n |^2 n^3$ as a function of n and for $\omega_1=\omega_2$ in order to visualize the convergence towards the threshold probability. Also in this case, the calculations have been performed in both gauges with good agreement (within 1%). Fig. 6 shows how the threshold probability converges towards a finite value, which has been computed by a polynomial extrapolation.

Similar calculations have been performed for a number of frequencies up to the first resonance at $0.75R$. In Fig. 7, we display the values of the threshold probability W_1^t as a function of the frequency $\nu_1=\omega_1/R$ for $0.5 \leq \nu_1 \leq 0.75$. The two-photon transparency occurs at $\nu_1 \approx 0.68$. A selection of numerical values of w_1^t is presented in Table IV. It is of interest to observe that the threshold ionization line shape given in Fig. 7 is very similar to the line shapes of transitions to discrete levels. The two-photon transparency frequency shifts towards lower values with increasing final state principal quantum numbers. We expect that similar line shapes with two-photon transparency will occur also for transitions above the

ionization limit.

We finally mention that the line shape here described should be very similar to those for many electron atoms, particularly the alkali atoms. Detailed calculations have been performed for the ionization limit of rare-gas atoms,[21] but unfortunately their accuracy is not sufficient to prove in this case the existence of two-photon transparency, because the results are strongly gauge dependent.

VIII. CONCLUSIONS

We can summarize the main results obtained in the present work as follows.

(i) Two-photon transition rates from the ground state of atomic hydrogen to any excited state of the discrete spectrum have been computed as functions of photon frequencies.

(ii) Gauge invariance of the transition rates can be verified only by using the complete set of intermediate eigenstates of hydrogen. The contribution from discrete and continuum spectrum are generally of the same order of magnitude. The contribution from the states of the discrete spectrum and those of the continuum are found to be completely different in the velocity and length gauges, this trend being more evident as one approaches the ionization limit.

(iii) Intermediate-state resonance enhancements produce a dramatic structure in the transition rates, which can be used to perform an intermediate-state spectroscopy of the hydrogen atom which will reveal hyperfine splitting, relativistic effects, and radiative corrections.

(iv) In correspondence to each resonance enhancement, we find a two-photon transparency.

(v) The two-photon threshold transition is obtained from a limiting process and shows a line shape similar to that of transitions to discrete levels.

(vi) Synchroton radiation appears as a particularly useful light source to verify the above points.

ACKNOWLEDGMENTS

One of the authors (F.B.) acknowledges the kind hospitality of the Department of Physics of the University of Illinois at Urbana, where part of this research was performed. The authors are indebted to M. Inguscio for communicating to us estimates of p-state hyperfine splitting in hydrogen, and they wish to thank N. K. Rahman for useful discussions. This work was supported in part by the Consiglio Nazionale delle Ricerche (Italy) through the contract P.U.L.S. (Programma per l' Utilizzazione della Luce di Sincrotrone).

---

*Present address: Scuola Normale Superiore, I-5600 Pisa, Italy.

[1]T. W. Hänsch, in *Nonlinear Spectroscopy,* proceedings of the International School of Physics "Enrico Fermi," course 64, Varenna, 1975, edited by N. Bloembergen (North-Holland, Amsterdam, 1977), p. 17; H. Walter, in *Laser Spectroscopy,* edited by H. Walter (Springer, Berlin, 1976), p. 1.

[2]J. E. Björkholm, in *Nonlinear Spectroscopy,* proceedings of the International School of Physics "Enrico Fermi", course 64, Varenna, 1975, edited by N. Bloembergen (North-Holland, Amsterdam, 1977), p. 138; N. Bloembergen and M. D. Levenson, in *High-Resolution Laser Spectroscopy,* edited by K. Shimoda (Springer, Berlin 1979), p. 315; G. Grynberg and B. Cagnac, Rep. Prog. Phys. 40, 791 (1977).

[3]For a detailed bibliography, see M. M. Salour, Ann. Phys. (N.Y.) 111, 364 (1978).

[4]E. I. Toader, Rev. Roum. Phys. 24, 453 (1980); J. Morellec, D. Normand, G. Mainfray, and C. Manus, Phys. Rev. Lett. 44, 1394 (1980).

[5]T. W. Hänsch, I. S. Shahin, and A. L. Schawlow, Phys. Rev. Lett. 27, 707 (1970); B. Cagnac, G. Grynberg, and F. Biraben, *ibid.* 32, 643 (1974); J. E. Björkholm and P. F. Liao, *ibid.* 33, 128 (1974).

[6]T. W. Hänsch, S. A. Lee, R. Wallenstein, and C. Wieman, Phys. Rev. Lett. 34, 307 (1975); S. A. Lee, R. Wallenstein, and T. W. Hänsch, *ibid.* 35, 1262 (1975).

[7]F. Bassani, A. Quattropani, and J. -J. Forney, Phys. Rev. Lett. 39, 1070 (1977).

[8]D. A. Van Baak, B. O. Clark, and F. M. Pipkin, Phys. Rev. A 19, 787 (1979); B. O. Clark, D. A. van Baak, S. R. Lunden, and F. M. Pipkin, *ibid.* 19, 802 (1979).

[9]J. -J. Forney, A. Quattropani, and F. Bassani, Nuovo Cimento B 37, 78 (1977); Y. Aharanov and C. K. Au, Phys. Rev. A 20, 1553 (1979).

[10]A. Quattropani and R. Girlanda, Solid State Commun. 38, 1041 (1981); R. Girlanda, A. Quattropani, and P. Schwendimann, Phys. Rev. B 24, 2009 (1981).

[11]W. Gordon, Ann. Phys. (Leipzig) 2, 1031 (1929).

[12]H. A. Bethe and E. E. Salpeter, *Quantum Mechanics of One- and Two-Electron Atoms* (Springer, Berlin, 1957).

[13]A. Sommerfeld and G. Schur, Ann. Phys. (Leipzig) 4,

409 (1930).
[14]E. Arimando, M. Inguscio, and P. Violino, Rev. Mod. Phys. 49, 31 (1977); M. Inguscio (private communication).
[15]T. W. Hänsch, A. L. Schawlow, and G. Series, Sci. Am. 240, 3 (1979); 240, 72 (1979).
[16]A. I. Ferguson, J. E. M. Goldsmith, T. W. Hänsch, and E. W. Weber, in *Laser Spectroscopy IV,* edited by H. Walter and K. W. Rothe (Springer, Berlin, 1979), p. 31.
[17]V. S. Letokhov and V. P. Chebatayev, *Nonlinear Laser Spectroscopy* (Springer, Berlin, 1977).
[18]See, e.g., A. M. Bonch-Bruevich and V. A. Khodovi, Usp. Fiz. Nauk. 93, 71 (1967) [Sov. Phys.—Usp. 10, 637 (1968)].
[19]P. F. Liao and J. E. Björkholm, Phys. Rev. Lett. 34, 1 (1975).
[20]N. K. Rahman, J. Phys. B 12, 3229 (1979).
[21]M. P. Pindzola and H. P. Kelly, Phys. Rev. A 11, 1543 (1975); R. Moccia, N. K. Rahman, and A. Rizzo (unpublished) and private communication.